

# Hail Trend Estimation in Germany utilizing Radar-based Hail Tracks, Convective Parameters, and Machine Learning Techniques

Christian Sperka<sup>1\*</sup>, Markus Augenstein<sup>1</sup>, Mathis Tonn<sup>1</sup>, Simon Siedersleben<sup>3</sup>, Matthias Hackl<sup>3</sup>, Michael Kunz<sup>1,2</sup>

<sup>1</sup>Institute of Meteorology and Climate Research, Karlsruhe Institute of Technology (KIT), Karlsruhe, Germany;

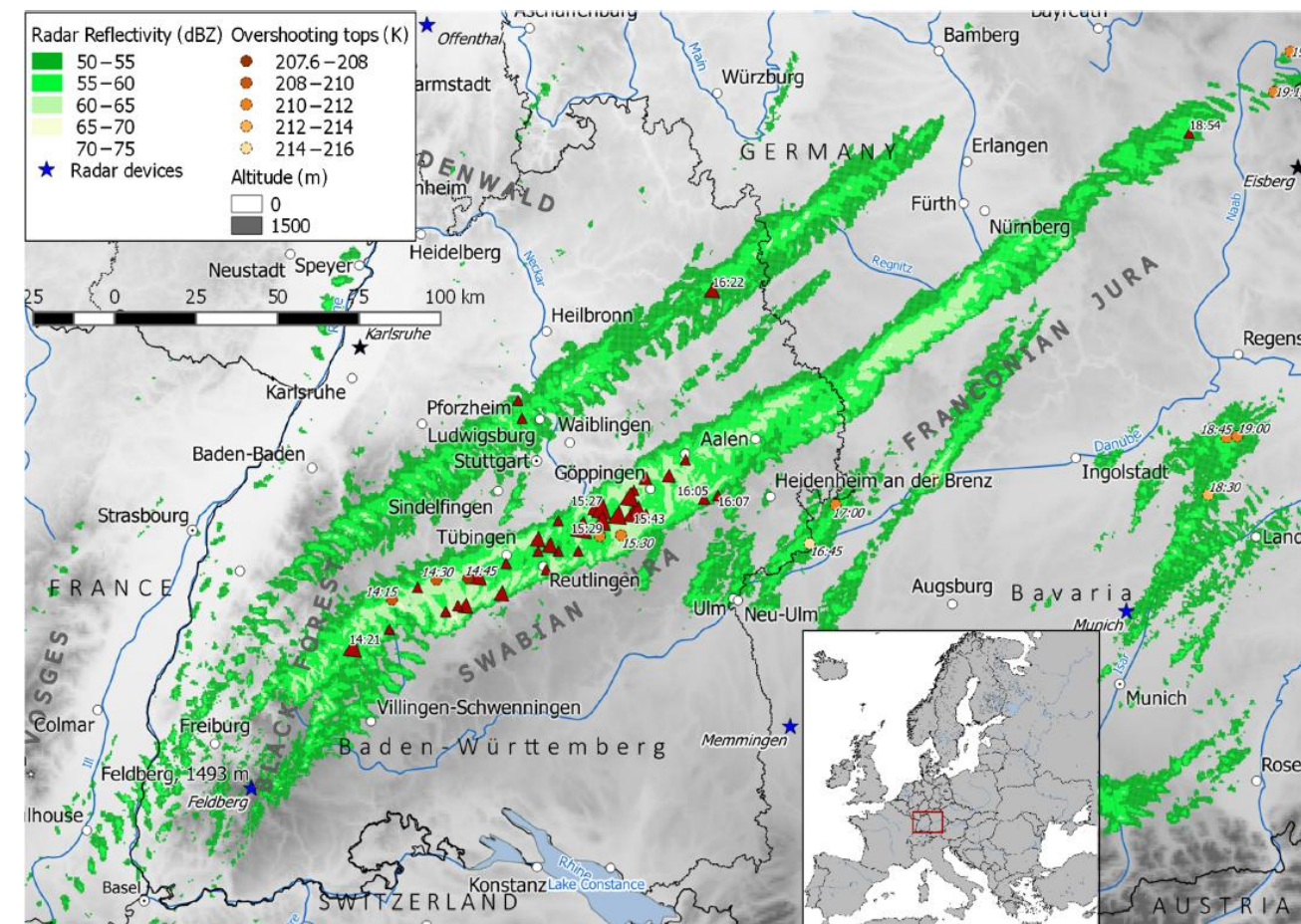
<sup>2</sup>Center for Disaster Management and Risk Reduction Technology (CEDIM), KIT;

<sup>3</sup>Allianz Reinsurance; \*: christian.sperka@kit.edu

## Motivation

### Research questions and overview:

- How have hail hazard and risk evolved over time in Germany?
  - To what extent can we predict past events solely with convective parameters derived from ERA5?
  - Which convective parameters are the drivers in recent changes in the frequency of convective storms?
- Past hail events are identified from radar reflectivity
- Machine learning (ML) methods, specifically U-Net architectures, are employed to predict our hail event catalogue based on convective parameters
- Hailstorms in Germany on 27-28 July 2013 caused a total economic loss of appr. EUR 3.6 billion [1] [2]
- How climate change affects frequency and severity of hail events is still not well understood [3]



## Data basis – Convective Parameters

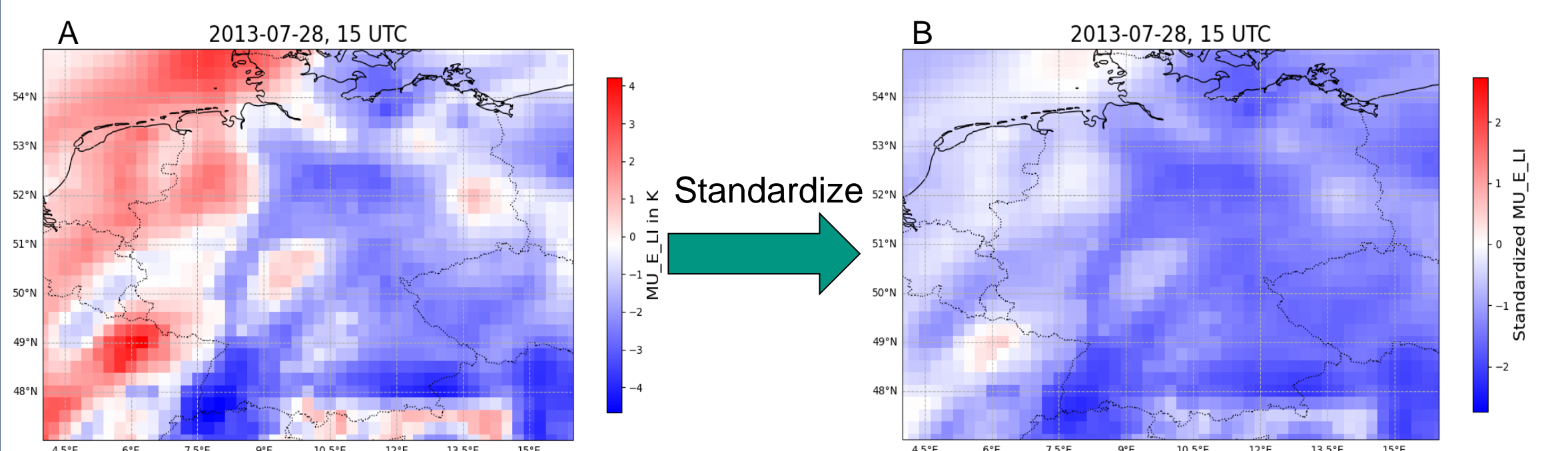
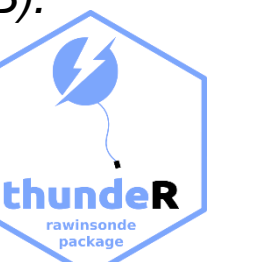


Fig. 1: Entraining Lifted Index at 500 hPa (A), standardized values via z-score standardization (B).

- Convective parameters calculated from ERA5 with thundeR [4]
- All parameters are standardized before their use in the ML model



## Data basis - Radar

- 3D radar data of German Weather Service (DWD)
- Summer period (AMJJAS) 2005 – 2024
- Potential hail tracks (PHTs) determined by cell tracking algorithm TRACE3D [5, 6]
- Track points are assigned to nearest grid points (3 x 3) on a regular 0.25° grid.

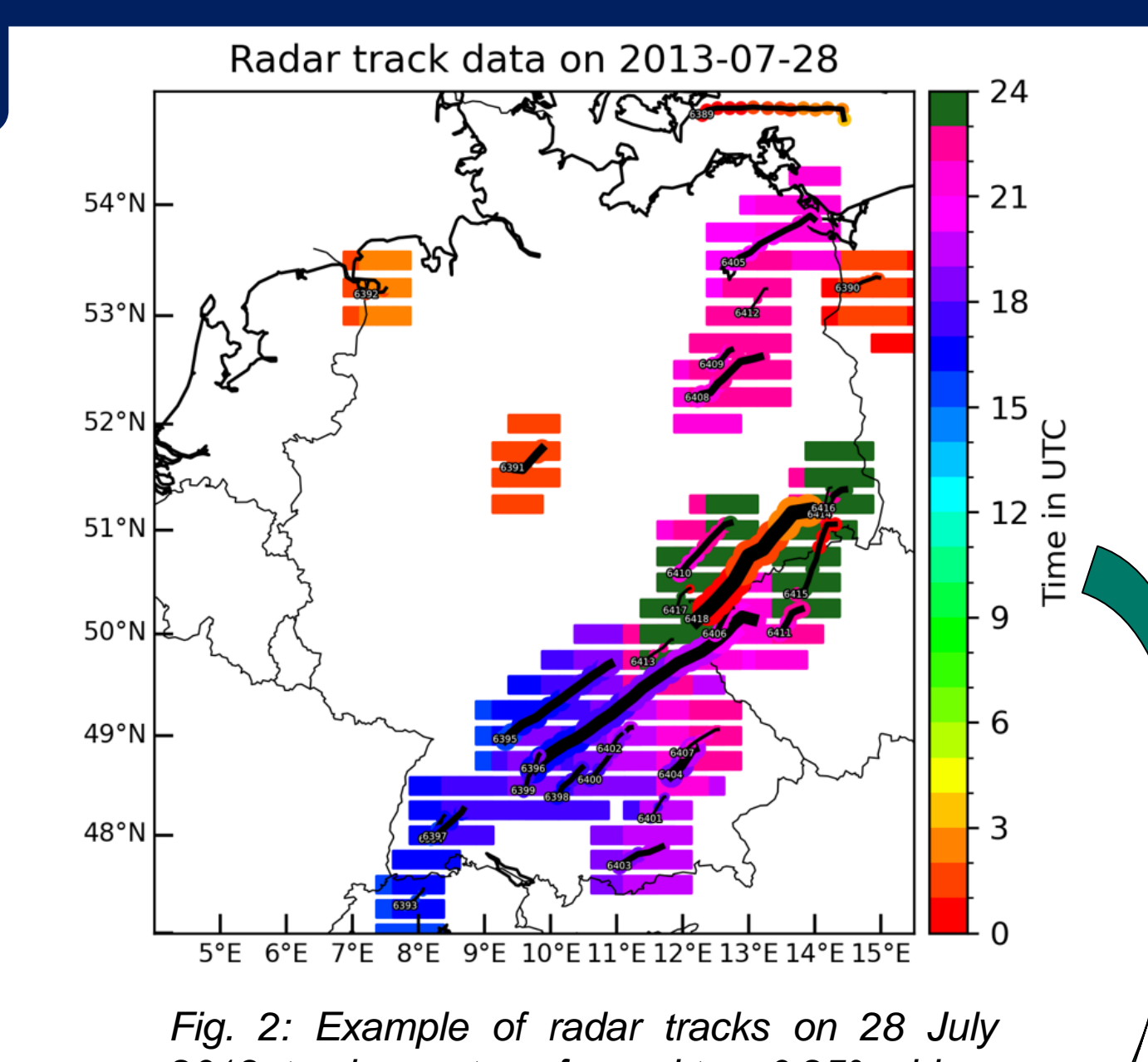


Fig. 2: Example of radar tracks on 28 July 2013; tracks are transformed to a 0.25° grid.

## Observed Climatology and Trends

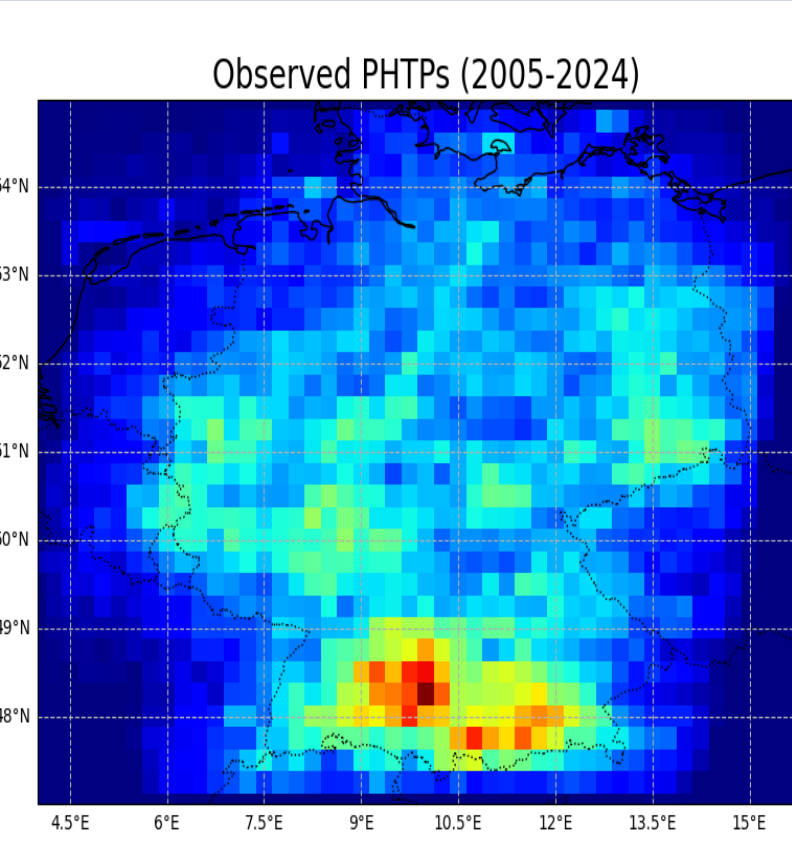


Fig. 3: Number of all Potential Hail Track Points (PHTPs) in summer half-year from 2005 – 2024 on a coarse 0.25° grid.

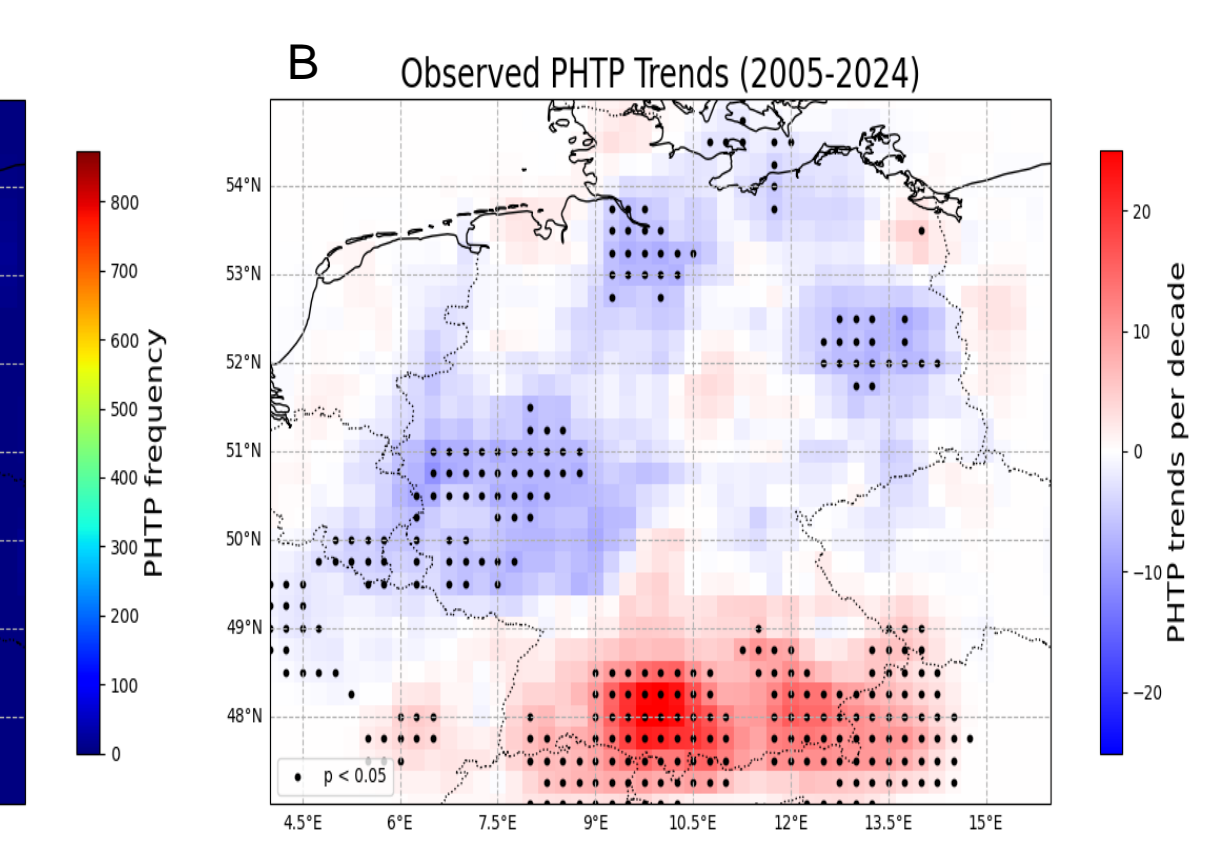
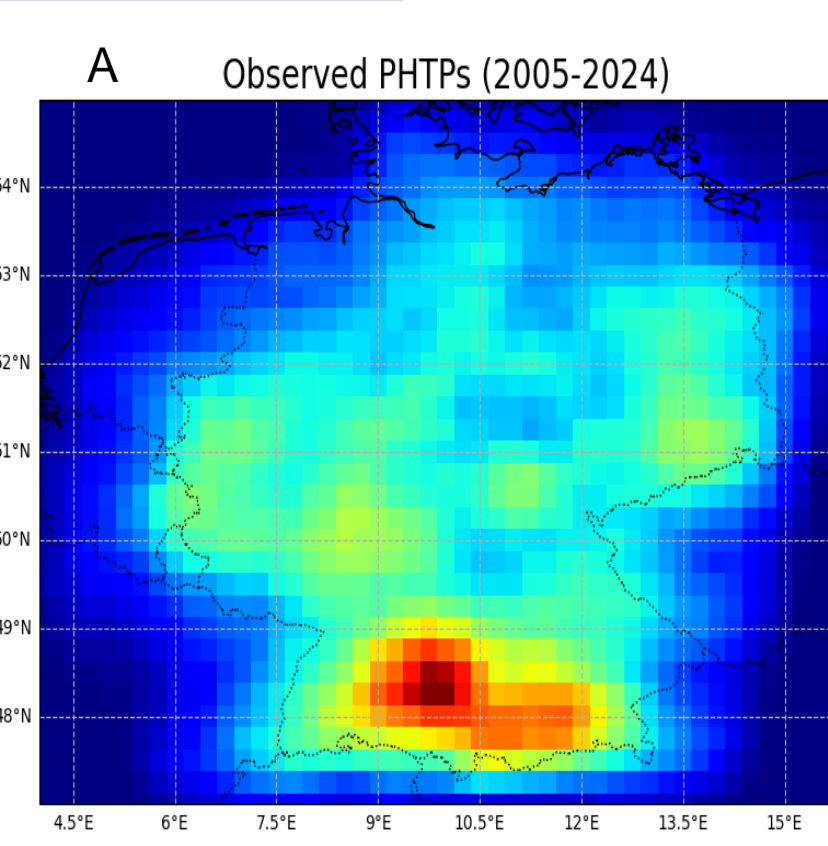


Fig. 4: (A) Climatology of smoothed (3 x 3) PHTPs in summer half-year from 2005 – 2024; (B) Trends of smoothed PHTPs from 2005 – 2024 per decade.

## U-Net Model Architecture

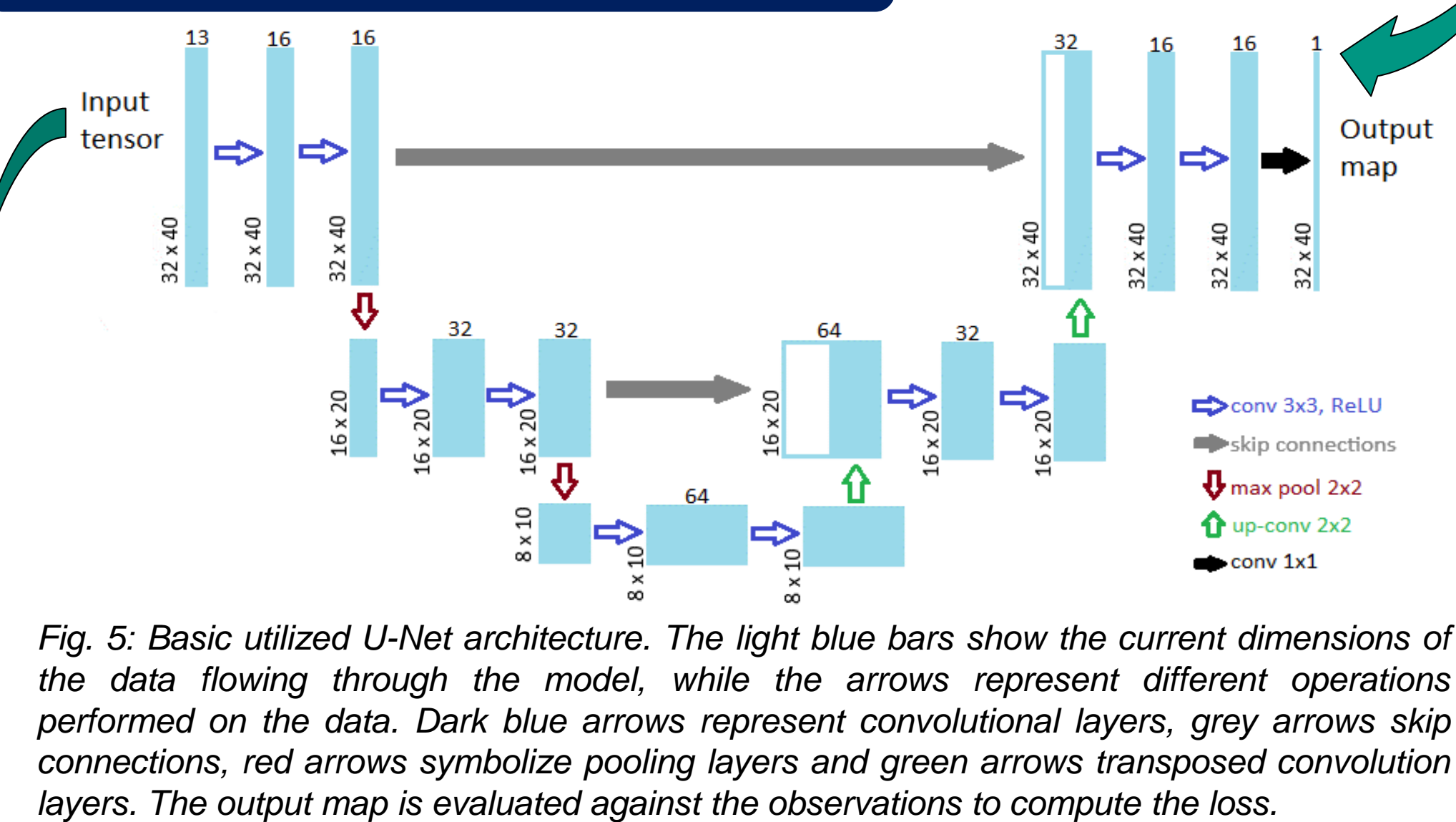


Fig. 5: Basic utilized U-Net architecture. The light blue bars show the current dimensions of the data flowing through the model, while the arrows represent different operations performed on the data. Dark blue arrows represent convolutional layers, grey arrows skip connections, red arrows symbolize pooling layers and green arrows transposed convolution layers. The output map is evaluated against the observations to compute the loss.

## Modeled Climatology and Trends

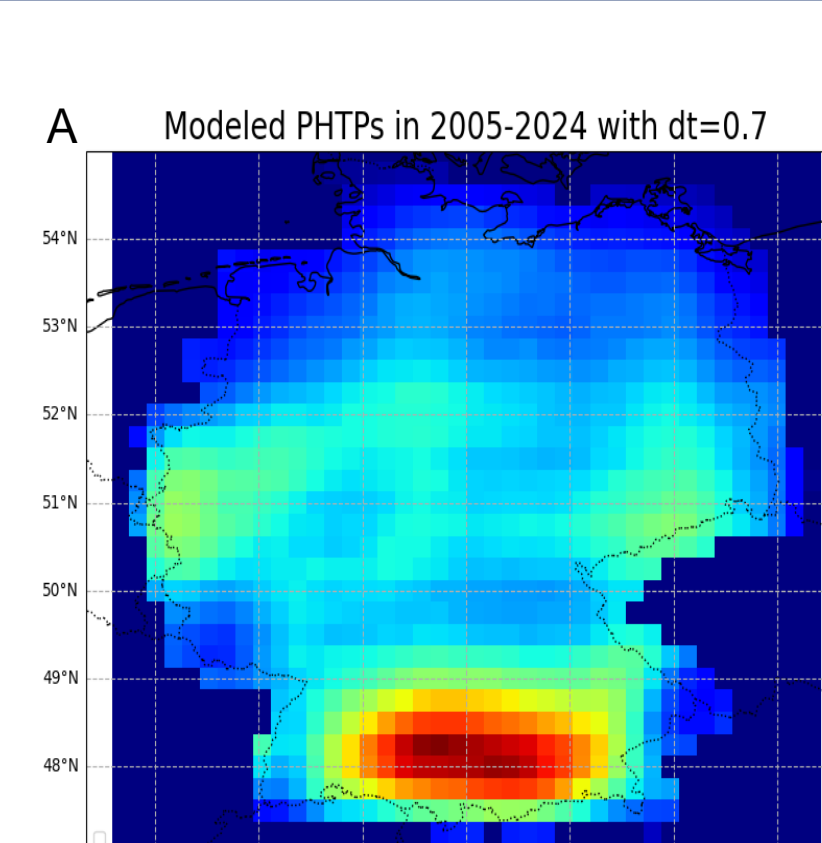


Fig. 6: (A) Modeled PHTP Climatology and (B) Trends of modeled PHTPs at decision threshold dt=0.7.

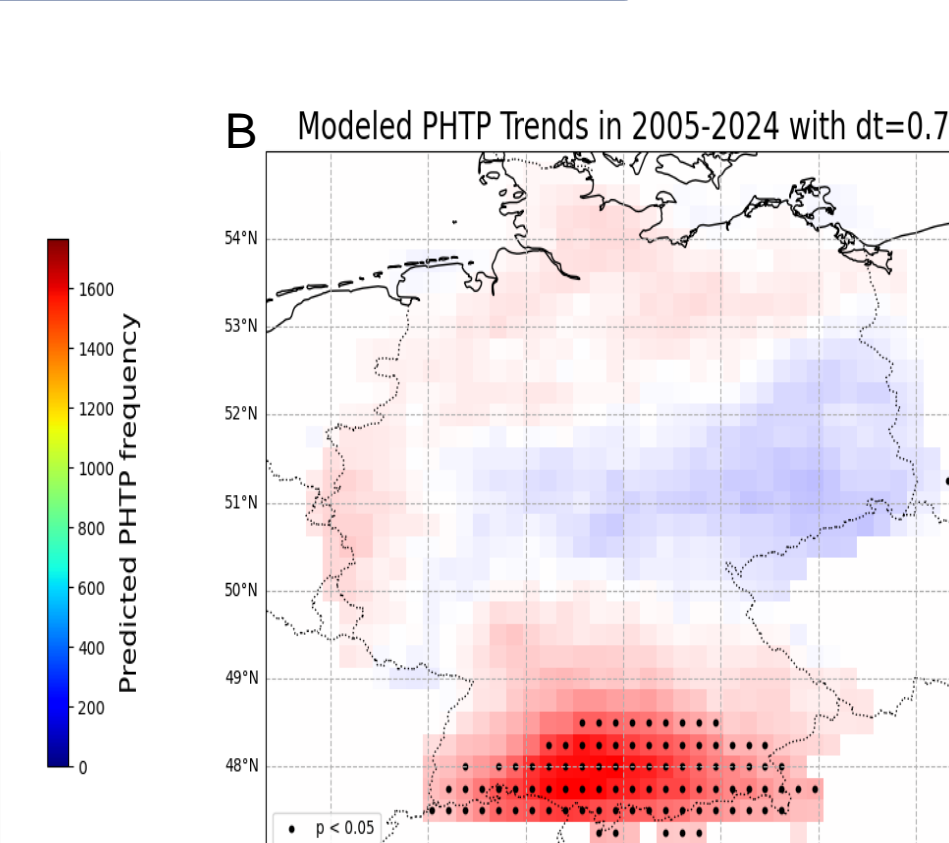


Fig. 7: Modeled trends with 2 additional aerosol variables, see Table 1 for detailed variable information.

## Input parameters

### Utilized variables in the model

Table 1: Variables used in the modeled climatology and trends (Figure 6). The two additional aerosol variables from CAMS global reanalysis [7] are used in the modeled trends in Figure 7.

Category	Parameter	Description
Thermo-dynamic	MU_E_LI MU_E_buoy_HGL THETA_E_MU_M10	Entraining lifted index at 500 hPa (Most-unstable parcel) Largest entraining parcel buoyancy in Hail Growth Layer (HGL) Difference in theta-e between MU parcel and -10°C isotherm height
Dynamic	BS_eff_MU Ventilation_16_km_RM SRH_eff_3km_RM SV_0500m_RM_G U_wind, V_wind IPV_320K Elevation	Effective shear between MU parcel initialization height and half of the distance to equilibrium level height Mean wind component perpendicular to 0-500 m AGL mean inflow axis, between 1 and 6 km AGL, for RM Bunkers vector Effective storm-relative helicity for 3 km layer with a base at MU parcel height, for RM Bunkers vector Mean streamwise vorticity between hodograph origin (0 m/s) and 500 m AGL, for RM Bunkers vector Zonal and meridional wind component (calculated from mean wind and dir in 0-6 km) Potential Vorticity on the $\theta = 320K$ level in PVU Height above sea level in m
Moisture	PRCP_WATER_eff Moisture_Flux_SR_eff	Effective precipitable water (entire column) accounting for relative humidity Mean effective storm-relative moisture flux for 500 m layer with a base at MUML parcel height
Aerosols	duaod550 suao550	Dust aerosol optical depth at 550 nm Sulphate aerosol optical depth at 550 nm

MU: most-unstable parcel based on highest theta-e between surface and 3 km

## Temporal Evolution

- Strong diurnal and seasonal cycle in observed PHTs
- ML model can replicate diurnal and seasonal cycles

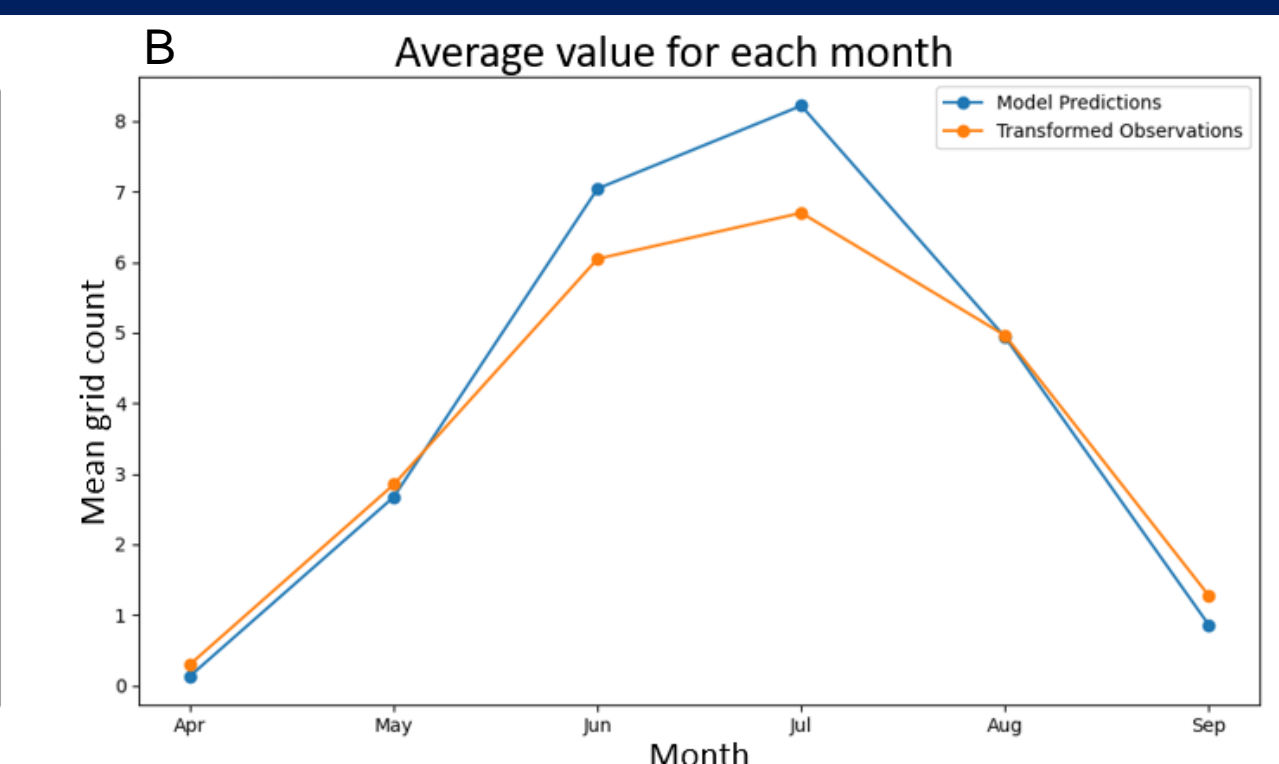
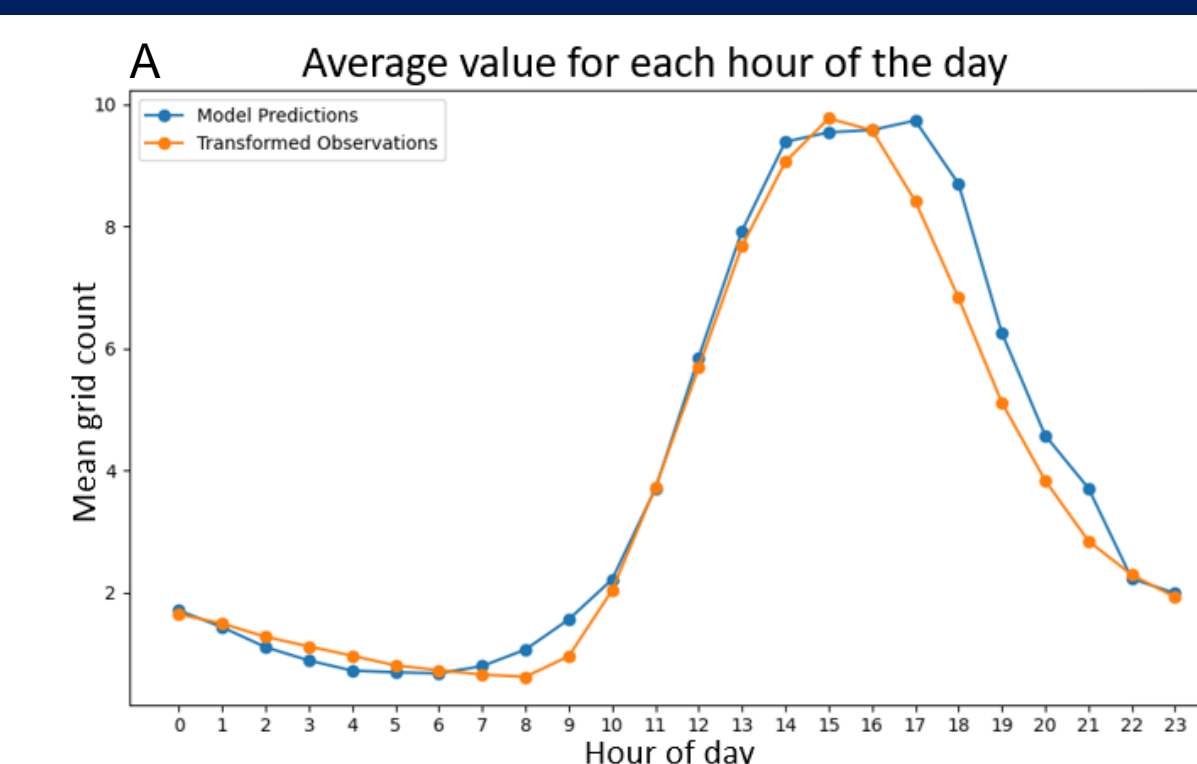


Fig. 8: Temporal evolution of observations (orange) and model predictions (blue) at decision threshold dt = 0.7 for diurnal (A) and monthly (B) cycles. All ML model predictions were divided by 1.5 to match the total amount of observed values.

## Dust effect on hail

- Medium levels of dust are favorable for hail
- Extreme values in lower levels of the atmosphere decrease hail probability

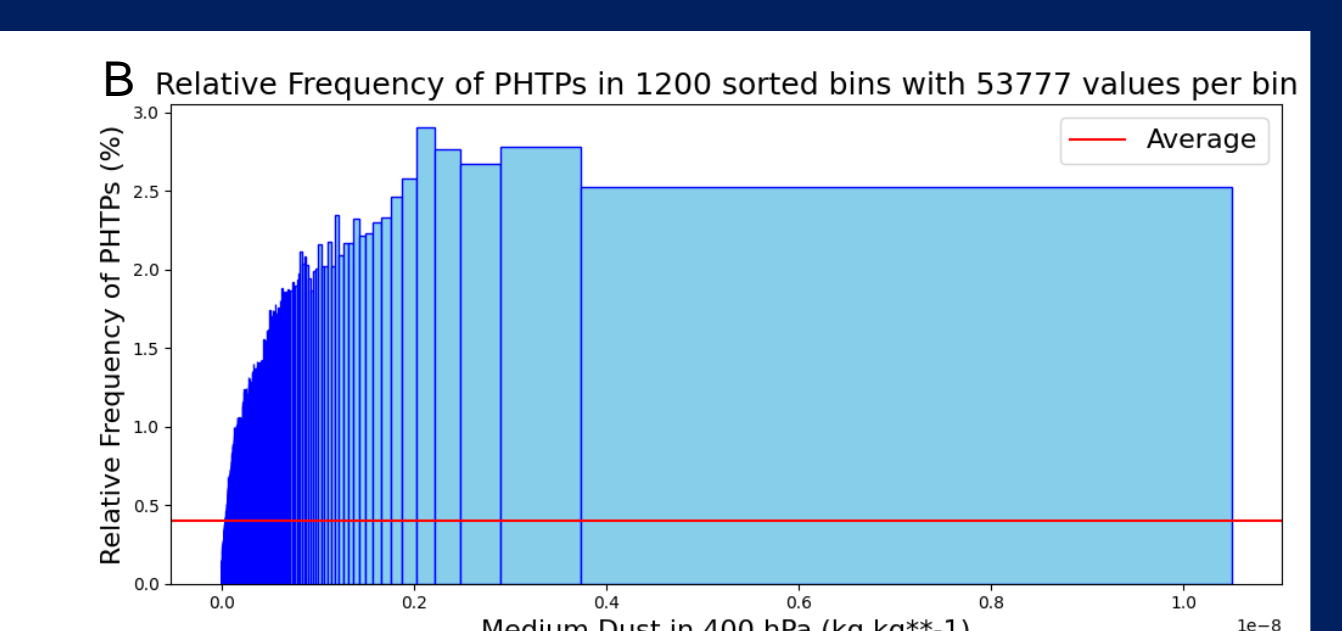
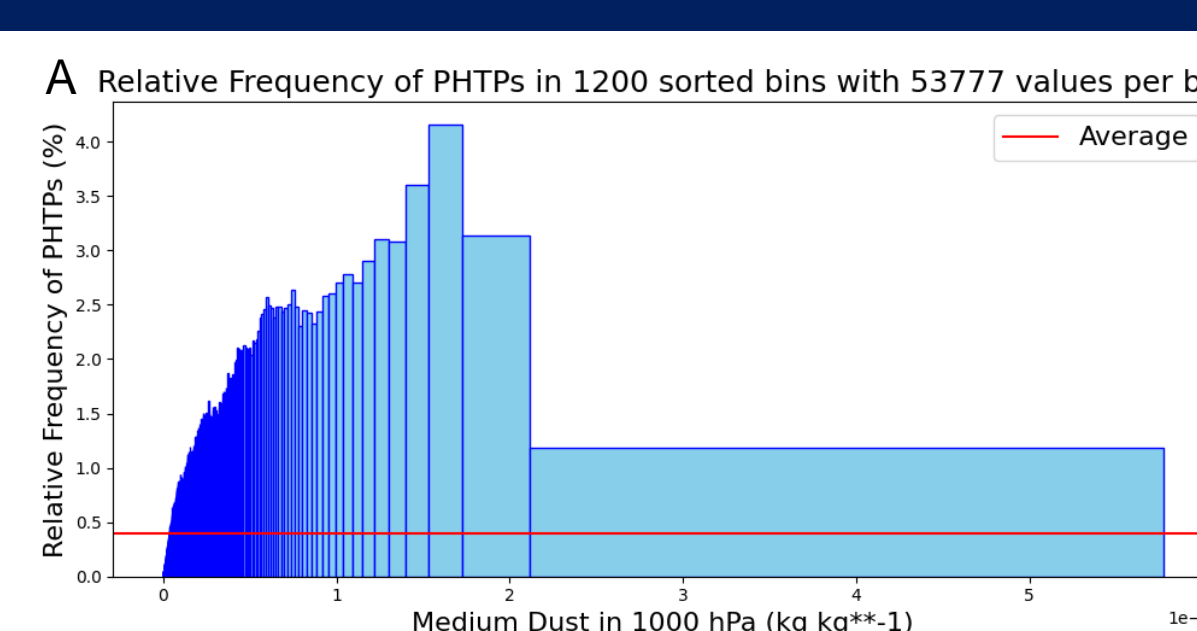


Fig. 9: Relative frequency of PHTPs for grid points with specific medium dust values in sorted bins that contain equal amounts of values at 1000 hPa (A) and at 400 hPa (B). Only data within Germany were used for this figure.

## Project outlook

- Analysis of trends in the past based on reanalysis data separated by hail intensity classes (based on hail size, cell track characteristics, insurance data)
- Further explore the effect of aerosols on hail
- Transfer of methods to an ensemble of regional climate models for different global warming levels
- Estimation of future trends of hail events

## Literature

- [1] Swiss Re (2014): Natural catastrophes and man-made disasters in 2013: large losses from floods and hail
- [2] Kunz, M., Blahak, U., Handwerker, J., Schmidberger, M., Punge, H.J., Mohr, S., Fluck, E. and Bedka, K.M. (2018), The severe hailstorm in southwest Germany on 28 July 2013: characteristics, impacts and meteorological conditions. Q.J.R. Meteorol. Soc., 144: 231-250. <https://doi.org/10.1002/qj.3197>
- [3] Raupach, T.H., O. Martius, J.T. Allen, M. Kunz, S. Lasher-Trapp, S. Mohr, K.L. Rasmussen, R.J. Trapp and Q. Zhang, 2021: The effects of climate change on hailstorms. nature Rev. Earth Environ., 2, 213–226, doi: 10.1038/s43017-020-00133-9
- [4] Taszarek, M., B. Czernecki, P. Szuster (2024): ThundeR – A rawinsonde package for processing convective parameters and visualizing atmospheric profiles
- [5] Handwerker, J. (2002): Cell tracking with TRACE3D – A new algorithm. Atmos. Res., 61, 15-34, doi: 10.1016/S0169-5018(05)00100-4.
- [6] Schmidberger, M. (2018): Hagelgefährdung und Hagelrisiko in Deutschland basierend auf einer Kombination von Radardaten und Versicherungsdaten. Dissertation, Wiss. Ber. des Ins. für Meteorologie und Klimaf., KIT, Vol. 78, doi: 10.5445/KSP/1000086012
- [7] Copernicus Atmosphere Monitoring Service (2020): CAMS global reanalysis (EAC4). Copernicus Atmosphere Monitoring Service (CAMS) Atmosphere Data Store, DOI: 10.24381/d58b47